



# Wind Power Plant Enhancement with a Fault-Current Limiter

## Preprint

E. Muljadi and V. Gevorgian  
*National Renewable Energy Laboratory*

F. DeLaRosa  
*Zenergy Power Inc.*

*To be presented at the IEEE PES Annual Meeting  
Detroit, Michigan  
July 24-29, 2011*

**NREL is a national laboratory of the U.S. Department of Energy, Office of Energy Efficiency & Renewable Energy, operated by the Alliance for Sustainable Energy, LLC.**

**Conference Paper**  
NREL/CP-5500-49781  
March 2011

Contract No. DE-AC36-08GO28308

## NOTICE

The submitted manuscript has been offered by an employee of the Alliance for Sustainable Energy, LLC (Alliance), a contractor of the US Government under Contract No. DE-AC36-08GO28308. Accordingly, the US Government and Alliance retain a nonexclusive royalty-free license to publish or reproduce the published form of this contribution, or allow others to do so, for US Government purposes.

This report was prepared as an account of work sponsored by an agency of the United States government. Neither the United States government nor any agency thereof, nor any of their employees, makes any warranty, express or implied, or assumes any legal liability or responsibility for the accuracy, completeness, or usefulness of any information, apparatus, product, or process disclosed, or represents that its use would not infringe privately owned rights. Reference herein to any specific commercial product, process, or service by trade name, trademark, manufacturer, or otherwise does not necessarily constitute or imply its endorsement, recommendation, or favoring by the United States government or any agency thereof. The views and opinions of authors expressed herein do not necessarily state or reflect those of the United States government or any agency thereof.

Available electronically at <http://www.osti.gov/bridge>

Available for a processing fee to U.S. Department of Energy and its contractors, in paper, from:

U.S. Department of Energy  
Office of Scientific and Technical Information

P.O. Box 62  
Oak Ridge, TN 37831-0062  
phone: 865.576.8401  
fax: 865.576.5728  
email: <mailto:reports@adonis.osti.gov>

Available for sale to the public, in paper, from:

U.S. Department of Commerce  
National Technical Information Service  
5285 Port Royal Road  
Springfield, VA 22161  
phone: 800.553.6847  
fax: 703.605.6900  
email: [orders@ntis.fedworld.gov](mailto:orders@ntis.fedworld.gov)  
online ordering: <http://www.ntis.gov/help/ordermethods.aspx>

Cover Photos: (left to right) PIX 16416, PIX 17423, PIX 16560, PIX 17613, PIX 17436, PIX 17721



Printed on paper containing at least 50% wastepaper, including 10% post consumer waste.

# Wind Power Plant Enhancement with a Fault-Current Limiter

**E. Muljadi**

Fellow, IEEE  
NREL  
1617 Cole Blvd.  
Golden, CO 80401,  
USA  
eduard.muljadi@nrel.gov

**V. Gevorgian**

Member, IEEE  
NREL  
1617 Cole Blvd.  
Golden, CO 80401,  
USA  
vahan.gevorgian@nrel.gov

**F. DeLaRosa**

Senior Member, IEEE  
Zenergy Power Inc.  
1616 Rollins Road  
Burlingame, CA 94010  
USA  
francisco.delarosa@zenergypower.com

**Abstract—** An important aspect of wind power plant (WPP) impact studies is to evaluate the short-circuit current (SCC) contribution of the plant into the transmission network under different fault conditions. This task can be challenging to protection engineers due to the topology differences between different types of wind turbine generators (WTGs) and the conventional generating units.

While it is important to size the circuit breaker to accommodate the available SCC, the available rating of a circuit breaker is limited. A fault-current limiter (FCL) has the capability to limit the SCC, and in some cases, may be necessary to limit the SCC from a WPP to defer the replacement of a circuit breaker currently installed in the transmission line.

This paper investigates the capability of a saturable core FCL to limit the SCC of different types of WTGs. Different faults are simulated to investigate the effectiveness of the FCL to limit the SCC and to reduce transient torque during faults. Several cases will be considered to demonstrate the benefits of using FCLs in unique situations.

**Index Terms** — Fault contribution, saturable core fault-current limiter, induction generator, protection, short circuit, wind power plant, wind turbine.

## I. INTRODUCTION

Energy and environmental issues have become one of the biggest challenges facing the world. In response to energy needs and environmental concerns, renewable energy technologies are considered the future technologies of choice [1], [2]. Renewable energy is harvested from nature, and it is clean and free. However, it is widely accepted that renewable energy is not a panacea that comes without challenges. With the federal government's aggressive goal of achieving 20% wind energy penetration by 2030, it is necessary to understand the challenges that must be overcome when using renewable energy.

In the years to come, there will be more and more wind power plants (WPPs) connected to the grid. With the goal of 20% wind penetration by 2030, the WPP's operation should be well planned. The power system switchgear and power system protection for WPPs should be carefully designed to be compatible with the operation of conventional synchronous generators connected to the same grid. This paper illustrates the behavior of short-circuit current (SCC) contributions for different types of WTGs.

### A. A Typical Wind Power Plant

As shown in Figure 1, a WPP consists of many (hundreds) of wind turbine generators (WTGs). Currently, available WTG sizes are between 1 MW and 5 MW. The WTG is connected at a low voltage level (e.g. 600 Volt), and a pad-mounted transformer is connected to step up the voltage to 34.5 kV.

Several turbines are strung together and connected in a

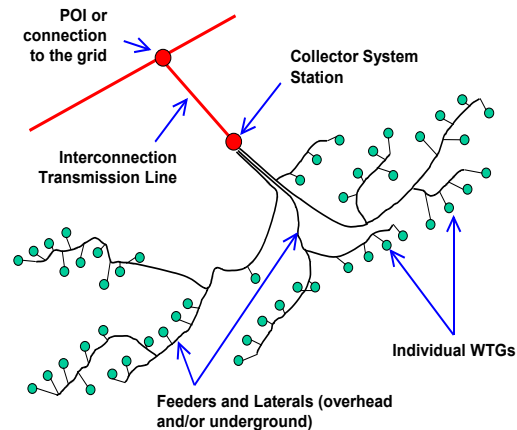


Figure 1. A typical WPP layout.

daisy chain fashion. The collector system is connected to the substation transformer where the voltage is stepped up to higher voltage (e.g., 230 kV) and the power is transmitted over long distance. Thus, a 300-MW wind power plant may consist of 300 turbines connected to the grid.

In this paper, the fault-current limiter (FCL) is proposed to be installed at the collector side (34.5 kV) of the substation transformer. Thus, the FCL will be able to protect the entire WPP.

### B. Organization of the Paper

The organization of this paper is as follows; in section II, the FLC description and method of operation will be covered. In section III, the SCC characteristics of different WTG types will be presented. In section IV, the characteristics of different faults will be discussed. While in section V, the effectiveness of FCLs will be presented. Finally, in section VI, the conclusion will summarize the paper findings.

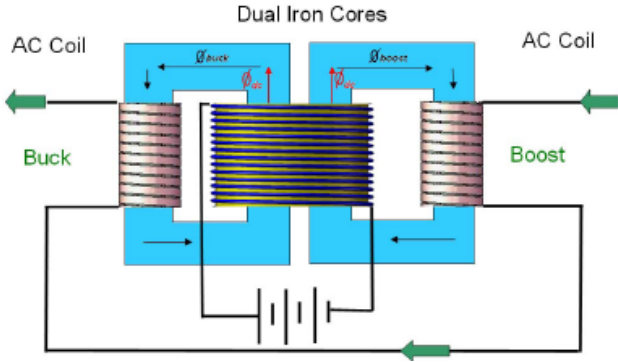


Fig.2. Dual iron cores saturated by an HTS DC-coil in a single-phase FCL, adapted from [3].

## II. FAULT CURRENT LIMITER

### A. Principle of Operation

The saturable core FCLs [3] consist of a set of coils wound around one or more ferromagnetic cores. A high-temperature superconducting (HTS) magnet is coupled to the core region in such a way that the DC magnetization force can saturate the magnetic material. As shown in Figure 2, each AC phase consists of two coils connected in series and wound around two core regions. Under normal operating conditions, the operating point on the  $\Phi$ - $I$  curve is always in the saturated region due to the DC bias, as depicted in Figure 3(a). AC positive flux shifts the operation point further into the saturated region due to the magnetic field of one of the AC coils that boosts the existing DC bias. The other AC coil has an opposite effect and its magnetic field and bucks the existing DC bias. All this happens in the region shaded in green in Figure 3(a), where the slope of the curve and therefore the resultant inductance of the FCL is very small. Under a fault, the operating point on the  $\Phi$ - $I$  plane is transitioned through the high slope, and therefore high inductance regions, as illustrated in red in Figure 3(a).

The corresponding flux changes in each of the coils are shown in Figure 3b under normal conditions and in Figure 3c under short-circuit conditions.

The total voltage  $E$  is shown as the thick line in Figures 3d and 3e, where the unsymmetrical portions cancel each other. Note that there is a  $90^\circ$  phase shift between the generated voltage and the flux changes.

$$e_{total} = e_{buck} + e_{boost}$$

$$\text{where: } e = \frac{\Delta\Phi}{\Delta t}$$

The corresponding voltages generated across the coils are shown in Figure 3d. As shown in Figure 3d, the generated

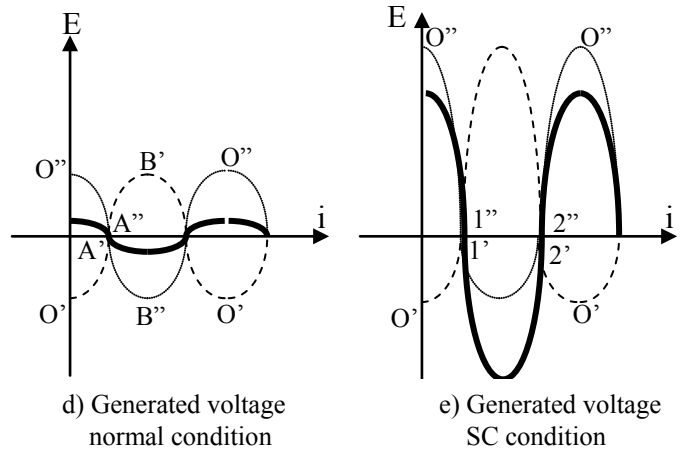
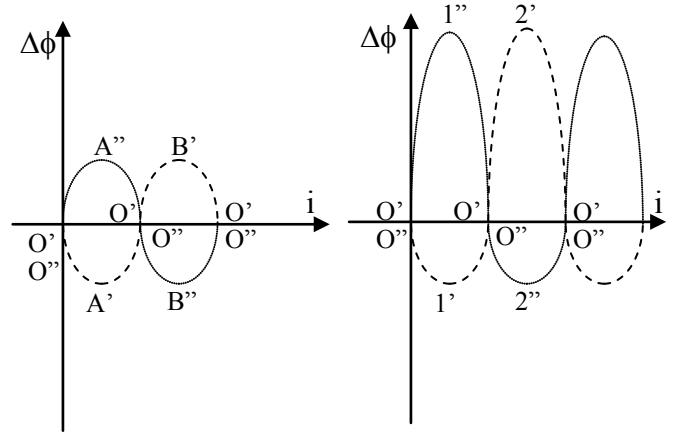
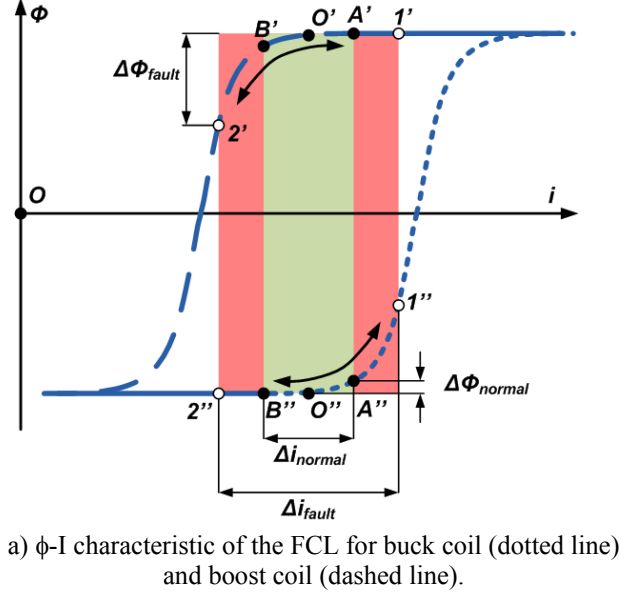


Figure 3. Operating region for normal and short-circuit conditions.

voltage in the boost coil and buck coil are symmetrical, and from the series connection of the coils and the way they were connected, the total generated voltage ( $E$ ) across the series coils is the sum of both voltages generated across each coil. The total voltage  $E$  is shown as the thick line. Note that there is a  $90^\circ$  phase shift between the generated voltage and the flux changes.

In the short-circuit condition, the SCC is very large, thus it drives the operating points to operate beyond the linear region of the  $\phi$ - $i$  curves. As shown in Figure 3a, the operating point moves along O'1'O'2'O'' in the  $\phi$ - $i$ , for the buck coil and similarly, the operating point moves along O'1'O'2'O' for the boost coil where the operation reaches outside the linear region. The corresponding flux changes in each of the coils is shown in Figure 3c. As shown in Figure 3c, the flux changes will be very large for the same amount of current change and the voltage drop across the FCL will also be very large.

As shown in Figure 3a, a very small change in the flux ( $\Delta\phi_{normal}$ ) is produced when the system operates under normal current because the operating points are in the saturation region of the magnetic circuit. The corresponding voltages generated across the coils are shown in Figure 3d. As shown in Figure 3d, the generated voltage in the boost coil and the buck coil are non symmetrical, however, from the series connection of the coils and the way they were connected, the total generated voltage ( $E$ ) across the series coils is the sum of the voltages generated across each coil.

On the other hand, the change in flux ( $\Delta\phi_{fault}$ ) is very large when a fault current is flowing in the coil. During the fault, the operating points are driven out of the saturation region into the linear region of the magnetic circuit, producing a large back EMF across the AC coils as depicted in Figure 3(e).

### B. Basic Equations in an FCL

The nonlinear model which describes the behavior of the device is based on the physical principle described above. The core material has  $B$ - $H$  characteristics that can be approximated by an inverse tangent function [3]. We begin by estimating the linkage magnetic field in the core section seen by one AC coil as

$$B(i_{ac}) = \frac{-2B_{sat}}{1 + \tan^{-1}(K\pi - \frac{\pi}{2})} [1 + \tan^{-1}(K \frac{\pi}{I_{max}} (I_{max} - i_{ac}) - \frac{\pi}{2})] + 2B_{sat}$$

where  $i_{ac}$  is the instantaneous AC line current,  $I_{max}$  is the line current it takes to fully saturate the cores, at which point the average magnetic field is  $B_{sat}$ , and  $K$  determines the range of line currents where the magnetic state of the cores are actively changing from saturated to unsaturated. The equation is scaled in such a way that  $B = B_{dc\_bias}$  at  $i_{ac} = 0$  (bias point, corresponding to point O' or O'' in Figure 3a), and the majority of the change in field occurs just before  $i_{ac} = I_{max}$ .

For a value of  $B_{sat} = 2.2$  Tesla, and  $I_{max} = 30$  kA, and two

different values of  $K$ , the differential flux density  $\Delta B(i_{ac})$  caused by AC currents is shown in Figure 4.

The effective inductance of an individual AC coil in the FCL can be computed as follows:

$$\tilde{L} = n_{ac} A_{core} \frac{\partial B(i_{ac})}{\partial i_{ac}}$$

Where  $\tilde{L}$  is the differential inductance,  $n_{ac}$  is the number of turns in the AC coil that carries the line current, and  $A_{core}$  is the cross-sectional area of the ferromagnetic core material. Figure 5 shows the plot of the differential inductance for different operating currents for  $K=2$  and  $K=5$ . In some cases, this model is improved by imposing two additional conditions. First,  $L$  must be greater than or equal to an additional parameter called  $L_{air}$  when the differential current  $\delta i_{ac}$  is small. This value represents the insertion impedance as an equivalent air-core inductance  $L_{air}$  corresponding to line "AO"B" or A'O'B" in Figure 3a. Furthermore, if  $\delta i_{ac}$  is greater than  $I_{max}$ , then  $L$  moves beyond the saturation region into linear magnetization region. This accounts for the fact that when the line current is very large, the FCL's magnetic core is reverse saturated and the impedance is once again approximately equal to the insertion impedance of an equivalent air-core inductor. Note that the inductance changes signifi-

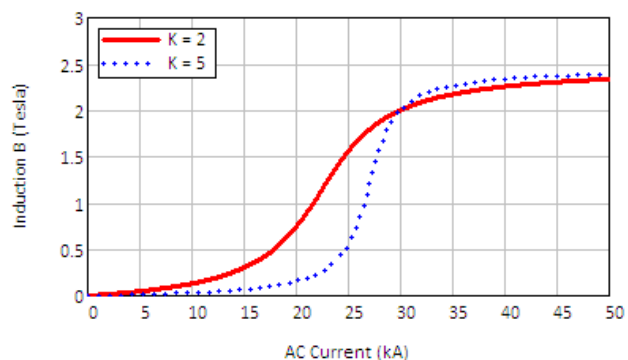


Fig. 4. The differential B(AC) for different operating currents.

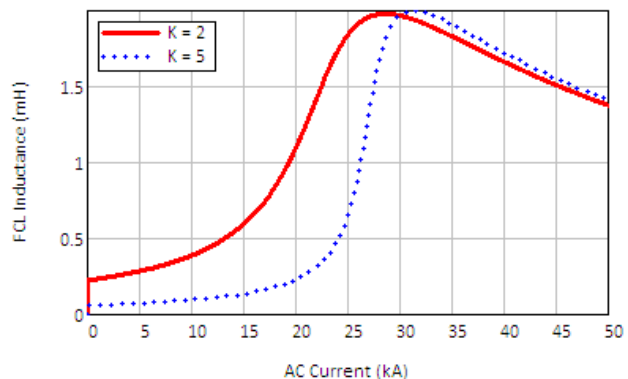


Fig. 5. The differential inductance for different operating currents.

cantly before the value of defined  $I_{max}$ .

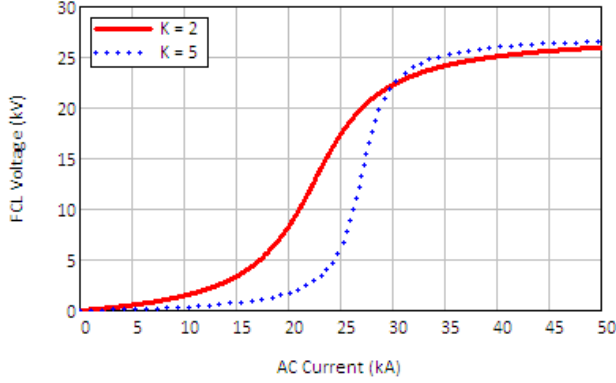


Fig. 6. Approximate voltage drop for different operating currents.

The induced voltage or back EMF across this section of the FCL is

$$V = L \frac{\partial i}{\partial t}$$

As shown in Figure 6, the voltage drop across the FCL varies depending on the operating point of the FCL.

The equations above provide a general framework for describing the behavior of an FCL in an electric circuit. This framework requires four input parameters:  $I_{max}$ ,  $B_{sat}$ ,  $K$ , and  $L_{air}$ . As shown in Figure 4 through Figure 6, the value of  $K$  influences the shape of the curve. The value of  $K$  is designed based on the dimensions, the characteristics of ferromagnetic material used (i.e., non linear relative permeability,  $\mu_r$ ), and the choice of the number of turns used for the AC coil. The characteristics can be shaped to satisfy the design criteria.

As described in the following sections, we use finite element method (FEM) simulations to calculate the average magnetic flux for various static values of superconducting currents and line currents. We then take these flux values and use a least-squares fitting procedure to determine the above parameters. Finally, we use some form of electrical simulation software (such as PSCAD®) to implement the nonlinear inductance model and compare it to experimental results from the extensive tests performed on the 15-kV FCL device [3].

### III. THE EFFECT OF FCLS ON SCC CONTRIBUTION FOR WTG TYPE 1 – INDUCTION GENERATOR

To investigate the impact of FCLs on SCC contribution, an FCL is installed in series with the line at the low voltage side of the substation transformer. In Figure 7, the single-line diagram of a typical WPP is shown [4]. With the insertion of the FCL, the SCC from all WTGs within the wind plant will be subjected to the change in FCL inductance due to the changes in current.

First, let us consider the WTG Type 1 (induction generator) used in the WPP investigated. The block diagram of the wind turbine Type 1 is shown in Figure 8.

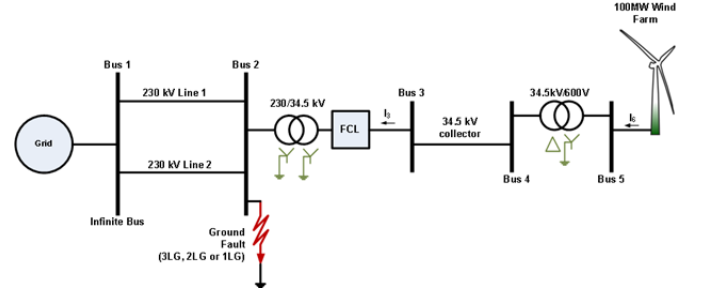


Fig. 7. FCL inserted at the low voltage side of a 34.5-kV substation transformer.

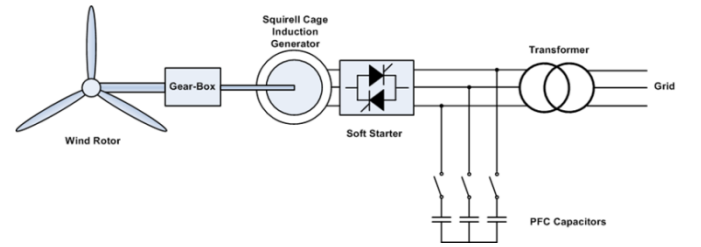


Fig. 8. Type 1 WTG.

#### A. Three Phase Faults

In this section, the aggregated contribution of all WTGs in a WPP is considered. The main difference between the characteristic of the three phase fault in a synchronous generator and an induction generator is the nature of field excitation. In a synchronous generator, the field winding is controlled by the field excitation and the field current continues to be present during the fault, generating the EMF voltage  $E$  driving the fault currents [5-6]. In an induction generator, when there is a three phase fault at the terminals, the voltage at the stator winding terminals drops to zero and there is no grid voltage available to maintain the magnetic flux. The magnetic flux in the air gap eventually dissipates as the fault progresses [7-9].

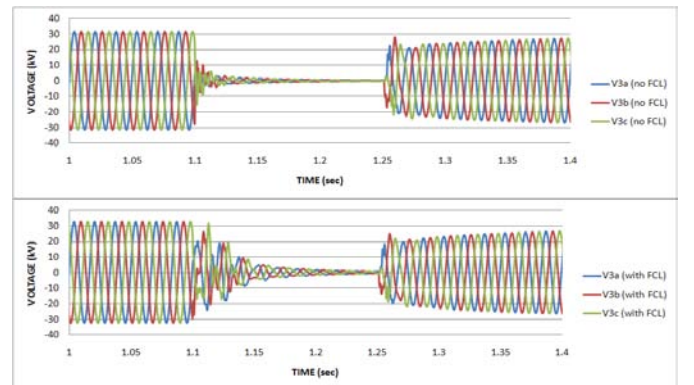


Fig.9. Voltage at the substation transformer for a three phase fault.

Figure 9 shows the voltage at the low voltage side of the substation transformer when the three phase fault occurs. As shown, the voltage quickly dies out when the three phase fault sustains for many cycles, however, when the FCL is inserted in series with the line, the voltage dies out in a longer time constant.

The fault currents of the two systems are compared. It is shown in Figure 10 that a significant current reduction is achieved when the FCL is installed. Without the FCL, the peak of the fault current reaches 10 kA. With the FCL installed, it can reduce the limit the peak of fault current down to 4 kA.

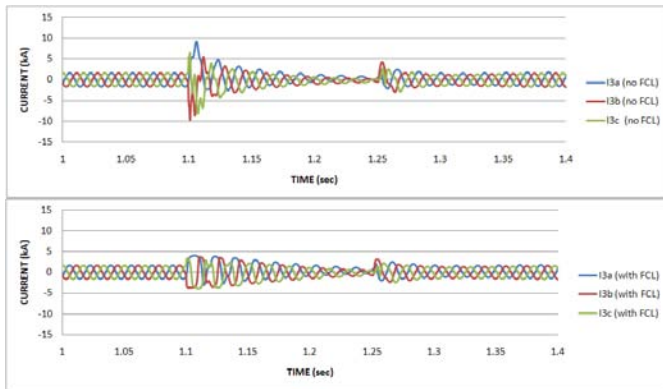


Fig. 10. Fault currents at the substation transformer for a three phase fault.

### B. Single line-to-ground (SLG) Fault

The single line-to-ground (SLG) fault has significant implications on WTG applications, especially for Type 1 and Type 2 machines. Under this type of fault, unequal current flows in the three phases and the unfaulted phases are still available to excite the generator fluxes. Thus, the system within the power plant is operated under unbalanced condition at 60 Hz operation until the fault is removed.

The FCL is represented as variable impedance in the diagram. Under an SLG fault, the FCL behaves differently among the three phases. The larger the current flow in any phase, the larger the apparent impedance of the FCL at that phase. As a result, it has a balancing impact on the overall system.

Figure 11 shows the system without the FCL and produces a larger fault current in the faulted line. The unbalanced series impedance among the three phases with the FCL is such that the system tends to have less fault current on the faulted line.

From Figure 11, the inductance in the faulted line (phase a) appears to be the largest among the three lines. It is also shown that due to the variation of the instantaneous inductance, the nonlinear variation due to the magnetic saturation creates a less than perfect sinusoidal current during the fault.

The comparison between the two simulations of an SLG fault with and without FCL in the circuit shows that the presence of the FCL in the circuit will create more balanced currents in the system during a fault event.

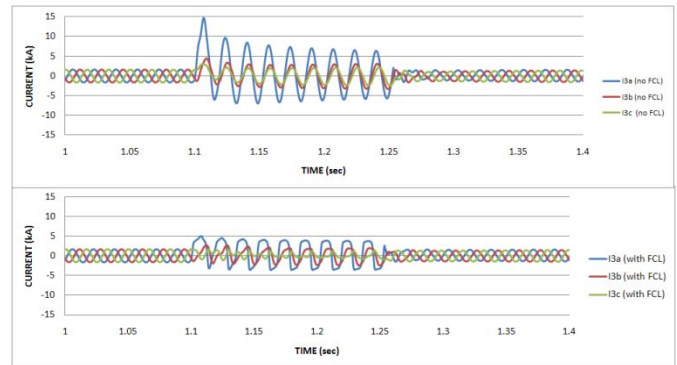


Fig. 11. Fault currents at the substation transformer for a single line-to-ground fault.

Figure 12 shows the three sequence currents (positive, negative, and zero sequence currents). The response of the system with and without FCL is shown on the same graphs.

It is shown that for the positive, negative, and zero sequence currents, there is a significant reduction of transient currents during the first few cycles during the faults. This reduction can significantly impact the transient torque production.

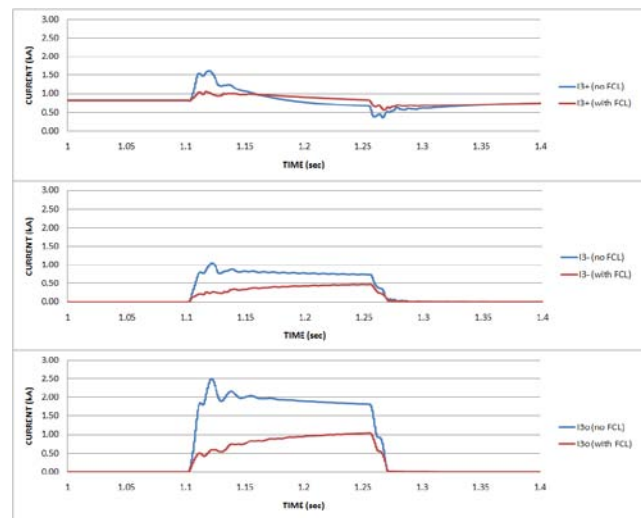


Fig.12. The sequence currents at the substation transformer

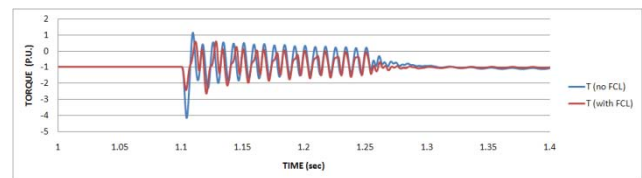


Fig. 13. The transient torque reduction with a FCL installed in the circuit.

The concept of minimizing unbalanced voltage on induction machines with unsymmetrical series components has been proven to be effective [10-11]. The same concept can be extended to a WPP by using a FCL at the substation transformer.

Figure 13 shows the impact of a FCL on the transient torque reduction in an induction generator during an SLG fault. As shown in the figure, there is a significant reduction in the fault current, as well as a significant reduction in the torque spike in the induction generator after the FCL is installed in series with the circuit.

In this operation, it is important to note that if the operation under unbalanced condition is left unnoticed, it may cause serious damage to the induction generator due to the unequal heating in the stator windings and the torque pulsations that may excite mechanical modes of the WTGs [12]. Although an unbalanced fault occurs for a very short duration, nevertheless, the resulting torque spike may damage the gear box from frequent faults that may occur in the lines.

#### IV. THE EFFECT OF FCL FOR DIFFERENT WTG TYPES

In this section, the SCC contributions of different WTGs for faults at the terminal of the generator are discussed. The three phase faults for different types of WTGs are short in duration because the air gap flux collapses without the support of sufficient terminal voltages. The duration of the fault is the longest for a Type 1 WTG.

Type 2 WTG has a lower SCC and a shorter time constant. The insertion of external rotor resistance into the rotor winding in the circuit reduces the SCC and the duration of the SCC.

Similarly, for a Type 3 WTG, the SCC and the duration of the three-phase-to-ground fault is shorter than for a Type 1 WTG. In a Type 3 WTG, there is a crowbar circuit that is used to protect the DC bus and the power switches in the power converter. The crowbar, in effect, adds adjustable effective rotor resistance and can even short circuit the rotor winding.

For a Type 4 wind turbine, the generator and grid is separated by a power converter. The power converter is limited by the current carrying capability of the power semiconductor used. Thus, the SCC contribution from a Type 4 wind turbine is limited to 110% of rated current (assuming temporary overload current is designed to be 110% rated). The SCCs from the WTG can be maintained in balance by controlling the power converter.

The SLG fault is the most likely to occur in the power grid. The terminal voltage and currents are sustained longer because the line voltages, except from one phase, are able to sustain air gap flux. The SC continues to flow until the fault is cleared.

The FCL is also installed in Type 2 and Type 3 WTGs and the reduction in SCCs and the torque transient are compared

between the system without FCL and the system with the FCL. The comparison in SCC reductions are tabulated in Table I, and the comparison in the transient torque reductions are tabulated in Table II. The values listed are the ratio of the values for systems with FCLs with respect to the values for systems without FCLs. The baseline used is the system without FCL, thus, values below 1.0 per unit indicate the reduction for the system with an FCL.

TABLE I  
THE RATIO OF THE SCC WITH AND W/O FCL  
FOR DIFFERENT TYPES OF WTGS

	TYPE 1	TYPE 2	TYPE 3
3LG	0.44	0.5	0.99
SLG	0.33	0.34	0.75
LL	0.47	0.38	0.71
LLG	0.33	0.36	0.70

TABLE II  
THE RATIO OF THE TRANSIENT TORQUES WITH AND W/O FCL  
FOR DIFFERENT TYPES OF WTGS

	TYPE 1	TYPE 2	TYPE 3
3LG	0.63	0.62	0.99
SLG	0.55	0.55	0.71
LL	0.66	0.63	0.77
LLG	0.66	0.65	0.67

#### V. CONCLUSIONS

In this paper, the role of FCLs is described in detail for Type 1 WTG. From section III, it is shown that the FCL can effectively reduce the SCC for the Type I wind turbine generator. It is also shown that for single line-to-ground and other types of unsymmetrical faults, the FCL behaves like an equalizer such that not only the reduction in the positive, negative, and zero sequence currents are achieved, but also the timing of the reduction is very beneficial. The most significant reduction of those sequence currents occurs during the transient (at the few cycles in the beginning of the faults), thus, as a result, the transient torque is reduced very significantly.

In section IV, the SCC contribution for different types of WTGs is tabulated as the ratio of SCC for a WPP with FCLs to the SCC for a WPP without FCLs. A table showing the reduction in transient torque for different faults and different WTGs is also tabulated in the same fashion. As shown in both tables, there is significant improvement in the SCC and the transient torque reductions for a WPP with FCLs.

The designs of the FCL for different types of WTGs must be designed specific to the WTG technology because the nature of the SCC contribution is unique for each type of WTG.

## VI. ACKNOWLEDGMENT

This work is supported by the U.S. Department of Energy and California Energy Commission.

## VII. REFERENCES

- [1] U.S. Department of Energy – Energy Efficiency and Renewable Energy, “20% Wind Energy by 2030 – Increasing Wind Energy’s Contribution to U.S. Electricity Supply,” May, 2008.
- [2] J. Charles Smith, Michael R. Milligan, Edgar A. DeMeo and Brian Parsons, "Utility wind Integration and operating impact state of the art," *IEEE Trans. Power Systems*, vol. 22, pp. 900-908, Aug. 2007.
- [3] Moriconi, F., Koshnick, N., De La Rosa, F. and Singh, A., “Modeling and Test Validation of a 15 kV 24 MVA Superconducting Fault Current Limiter”, in *Proc. of IEEE/PES Transmission and Distribution Conference*, New Orleans, USA, April 2010.
- [4] WECC Modeling and Validation Work Group, “WECC Wind Power Plant Power Flow Modeling Guide Prepared.” May 2008.
- [5] Short-circuit currents in three-phase a.c. systems–Part 0: Calculation of currents, IEC Standard 60909-0, July 2001.
- [6] IEEE Application Guide for AC High-Voltage Circuit Breakers Rated on a Symmetrical Current Basis, IEEE Standard C37.10-2000, Sept. 2000.
- [7] J. Moren, S.W.H. de Haan, “Short-Circuit Current of Wind Turbines with Doubly Fed Induction Generator,” *IEEE Transactions on Energy Conversion*, Vol. 22, No. 1, March 2007.
- [8] IEEE PES Wind Plant Collector System Design Working Group, “Power Transformer Application for Wind Plant Substation,” *Proceedings of the 2009 IEEE Power and Energy Society General Meeting*.
- [9] V. Gevorgian, E. Muljadi, " Wind Power Plant Short-Circuit Current Contribution for Different Fault and Wind Turbine Topologies", Presented at the 9th International Workshop on Large Scale of Wind Power into Power Systems, Quebec City, Quebec, Canada, July 18-19, 2010
- [10] E. Muljadi, R. Schiferl, and T.A. Lipo, "Unsymmetrical Triggering of Phase Back Controller for Unbalanced Operation of Induction Machine", *IEEE Transactions on Industry Applications*, Vol. IA-21, No. 4, May/June 1985, pp. 669- 677
- [11] J. Oyama, F. Profumo, E. Muljadi and T.A. Lipo, " Design and Performance of a Digitally Based Voltage Controller for Correcting Phase Unbalance in Induction Machines." *IEEE Transactions on Industry Applications* Vol. 26, No. 3, May/June 1990, pp. 425-433.
- [12] E. Muljadi, T.Batan, D.Yildirim, C.P. Butterfield, "Understanding the Unbalanced-Voltage Problem in Wind Turbine Generation," *IEEE-Industry Applications Society Annual Conference*, October 3-7, 1999 in Phoenix, Arizona.

## VIII. BIOGRAPHIES

**Eduard Muljadi** (M’82-SM’94-F’10) received his Ph. D. (in Electrical Engineering) from the University of Wisconsin, Madison. From 1988 to 1992, he taught at California State University, Fresno, CA. In June 1992, he joined the National Renewable Energy Laboratory in Golden, Colorado. His current research interests are in the fields of electric machines, power electronics, and power systems in general with emphasis on renewable energy applications. He is member of Eta Kappa Nu, Sigma Xi and a Fellow of the IEEE. He is involved in the activities of the IEEE Industry Application Society (IAS), Power Electronics Society, and Power and Energy Society (PES).

He is currently a member of various committees of the IAS, and a member of the Working Group on Renewable Technologies and Dynamic Performance Wind Generation Task Force of the PES. He holds two patents in power conversion for renewable energy.

**Vahan Gevorgian** (M’97) graduated from the Yerevan Polytechnic Institute (Armenia) in 1986. During his studies, he concentrated on electrical machines. His thesis research dealt with doubly-fed induction generators for stand-alone power Systems. He obtained his Ph.D. degree in electrical engi-

neering from the State Engineering University of Armenia in 1993. His dissertation was devoted to a modeling of electrical transients in large wind turbine generators.

Dr. Gevorgian is currently working at the National Wind Technology Center (NWTC) of National Renewable Energy Laboratory (NREL) in Golden, Colorado, USA, as a research engineer. His current interests include modeling and testing of various applications of small wind turbine based power systems.

**Francisco DeLaRosa** (M’91, SM’00) joined Zenergy Power Inc. in April 2008 as Director of Electrical Engineering. Before joining Zenergy Power, Inc., Francisco had held various positions in R&D, consultancy and training in the electric power industry for around 30 years. Francisco holds a PhD degree in Electrical Engineering from Uppsala University, Sweden. He is a Collective Member of CIGRE and a Senior Member of IEEE PES where he contributes in several WG’s including the TF on FCL Testing. His main interests include the assessment and integration of new technologies in the electric power system.

# REPORT DOCUMENTATION PAGE

Form Approved  
OMB No. 0704-0188

The public reporting burden for this collection of information is estimated to average 1 hour per response, including the time for reviewing instructions, searching existing data sources, gathering and maintaining the data needed, and completing and reviewing the collection of information. Send comments regarding this burden estimate or any other aspect of this collection of information, including suggestions for reducing the burden, to Department of Defense, Executive Services and Communications Directorate (0704-0188). Respondents should be aware that notwithstanding any other provision of law, no person shall be subject to any penalty for failing to comply with a collection of information if it does not display a currently valid OMB control number.

**PLEASE DO NOT RETURN YOUR FORM TO THE ABOVE ORGANIZATION.**

<b>1. REPORT DATE (DD-MM-YYYY)</b> March 2011		<b>2. REPORT TYPE</b> Conference Paper		<b>3. DATES COVERED (From - To)</b>	
<b>4. TITLE AND SUBTITLE</b> Wind Power Plant Enhancement with a Fault-Current Limiter: Preprint				<b>5a. CONTRACT NUMBER</b> DE-AC36-08GO28308	
				<b>5b. GRANT NUMBER</b>	
				<b>5c. PROGRAM ELEMENT NUMBER</b>	
<b>6. AUTHOR(S)</b> V. Gevorgian, E. Muljadi, and F. DeLaRosa				<b>5d. PROJECT NUMBER</b> NREL/CP-5500-49781	
				<b>5e. TASK NUMBER</b> WE11.0825	
				<b>5f. WORK UNIT NUMBER</b>	
<b>7. PERFORMING ORGANIZATION NAME(S) AND ADDRESS(ES)</b> National Renewable Energy Laboratory 1617 Cole Blvd. Golden, CO 80401-3393				<b>8. PERFORMING ORGANIZATION REPORT NUMBER</b> NREL/CP-5500-49781	
<b>9. SPONSORING/MONITORING AGENCY NAME(S) AND ADDRESS(ES)</b>				<b>10. SPONSOR/MONITOR'S ACRONYM(S)</b> NREL	
				<b>11. SPONSORING/MONITORING AGENCY REPORT NUMBER</b>	
<b>12. DISTRIBUTION AVAILABILITY STATEMENT</b> National Technical Information Service U.S. Department of Commerce 5285 Port Royal Road Springfield, VA 22161					
<b>13. SUPPLEMENTARY NOTES</b>					
<b>14. ABSTRACT (Maximum 200 Words)</b> This paper investigates the capability of a saturable core fault-current limiter to limit the short circuit current of different types of wind turbine generators. Different faults are simulated to investigate the effectiveness of the FCL to limit the SCC and to reduce transient torque during faults. Several cases will be considered to demonstrate the benefits of using FCLs in unique situations.					
<b>15. SUBJECT TERMS</b> Wind power plant; short circuit current; fault current; saturable core; voltage fault					
<b>16. SECURITY CLASSIFICATION OF:</b>			<b>17. LIMITATION OF ABSTRACT</b> UL	<b>18. NUMBER OF PAGES</b>	<b>19a. NAME OF RESPONSIBLE PERSON</b>
<b>a. REPORT</b> Unclassified	<b>b. ABSTRACT</b> Unclassified	<b>c. THIS PAGE</b> Unclassified			<b>19b. TELEPHONE NUMBER (Include area code)</b>

Standard Form 298 (Rev. 8/98)  
Prescribed by ANSI Std. Z39.18